

Measuring the Localization Length through the superconductor-insulator transition in ultrathin amorphous beryllium films

Wenhao Wu⁺ and E. Bielejec^{*}

⁺Department of Physics, Texas A&M University, College Station, Texas 77843

^{*}Sandia National Laboratories, Albuquerque, New Mexico 87185

Abstract

Electron transport and tunneling across the superconductor-insulator (SI) transition have been measured simultaneously for quench-condensed ultrathin amorphous beryllium films. The anomalous negative magnetoresistance previously observed in insulating films disappears when Mn impurities are introduced to the films, restoring a rather clean Efros-Shklovskii type hopping behavior. The combination of transport and tunneling data allows us to determine, *independently* and up to a constant on the order of unity, the localization length, ξ_L , and the dielectric constant, κ , for the films. As the normal-state sheet resistance of the films at 20 K is reduced with increasing film thickness, ξ_L increases exponentially. The SI transition occurs when ξ_L crosses the Ginzburg-Landau coherence length, ξ_S .

PACS Numbers: 74.25.Dw, 73.20.Fz, 71.30.+h, 72.20.Ee

Superconductivity in the presence of disorder has been a subject of great interest over the years [1]. In particular, recent discoveries [2,3] of the superconductor-insulator (SI) transitions in two-dimensions (2D), tuned by disorder or magnetic field are fascinating [4,5]. Theoretical studies of the effects of disorder on superconductivity date back to Anderson's theorem [6] which predicts that nonmagnetic impurities have no significant effect on superconductivity. However, this theorem does not consider the effect of Anderson localization. The scaling theory of localization [7] predicts that, in zero magnetic field, electronic wave functions are always localized in disordered 2D systems over a length scale called the localization length, ξ_L . Since superconductivity is a manifestation of long-range phase coherence of paired-electron states, the fundamental question is when and how superconductivity breaks down as the electronic states become strongly localized with increasing disorder.

A number of theories [8,9] have addressed this question. With increasing disorder, one expects that, when ξ_L becomes smaller than the size of a vortex core, the vortex core becomes an insulator. The vortex core could disintegrate because of large fluctuations in the phase of the superconducting order parameter. Robust superconductivity exists when $\xi_L > \xi_S$, where the Ginzburg-Landau coherence length, ξ_S , is a measure of the size of the vortex core. The other criterion [9] to consider is $[N(0)\xi_L^d]^{-1} < \Delta_S$, where $N(0)$ is the average density of states (DOS) at the Fermi energy, $d = 2$ is dimensionality, $[N(0)\xi_L^d]^{-1} = \Delta_L$ is the typical energy separation between localized states, and Δ_S is the Bardeen-Cooper-Schrieffer (BCS) gap. This condition means, if a localized system is divided into boxes of size ξ_L , there are on average a few localized states in each box with energies within Δ_S of the Fermi surface. These states can form a coherent local superconducting fluctuation. A superconducting ground state can be stabilized via inter-box Josephson tunneling established by localized states connecting adjacent boxes [10].

Recent studies of the SI transition have largely been motivated by experiments on ultrathin disordered superconducting films [2,3,11-14]. Many of these studies analyze the data following a scaling argument based on a Bose-Hubbard model [4] in which disorder drives a Bose-condensed superfluid into an insulating glass. However, this scaling theory does not address the microscopic origin of the SI transition. In this Letter, we investigate the interplay of localization and superconductivity in quench-condensed ultrathin

amorphous Be films of about 10 Å in thickness. We directly probe one of the most fundamental length scale of a disorder system, the localization length ξ_L , across the SI transition. ξ_L has been studied in a number of systems [15] by fitting the conductance to certain hopping laws. However, these experiments *do not* measure ξ_L directly. Rather, they measure the product $\xi_L\kappa$, where κ is the dielectric constant. In general, κ is not a constant and can change drastically near a phase transition. Here, we describe a procedure with which ξ_L and κ can be determined *independently* across the SI transition, based on simultaneous transport and tunneling measurements.

The Be films used for this study were thermally evaporated onto glass substrates held near 20 K. A multi-lead pattern with an area of 3×3 mm² between neighboring leads was pre-evaporated on the substrates. Details of our transport and tunneling measurements have been published earlier [14,16,17]. Figure 1 shows the sheet resistance, R_{\square} , versus $1/T^{1/2}$ on a semi-log plot for a set of Be films following an evaporation sequence to increase film thickness. Data in Fig. 1 show different behavior in two temperature regimes. At high temperatures, above 5 K, the curves appear to follow straight lines converging to about 10 k Ω/\square in the $T\rightarrow\infty$ limit. Below 5 K, R_{\square} increases much steeper with decreasing T for insulating films. These insulating films also show a puzzling magnetoresistance as we [16] have reported: the resistance can *decrease* by orders of magnitude with an increasing perpendicular field in the range of 2-10 T. Similar behavior was later observed in InOx films and was interpreted [18] as the field suppression of the super-insulating behavior due to a nonuniform Δ_S which leads to regions of large Δ_S interceded with regions of vanishingly small Δ_S , in analog to granular superconducting films. Since our magnetic field is not strong enough to completely suppress this super-insulating behavior in the Be films, we have recently introduced a small amount of Mn impurities to investigate the effect of magnetic impurities on the magnetoresistance. Mn was loaded in a tungsten basket, with the evaporation rate-current relation calibrated in a thermal evaporator at room temperature. The Mn source was mounted together with a Be source in a multi-source quench-condensation cell at the bottom of the IVC can of a dilution refrigerator. A mechanical shutter inside the dilution refrigerator, manually controlled from the top of the refrigerator, was used to open and close the Mn source during evaporation. The actual amount of Mn impurities deposited

on the Be films was too small to be registered by the quartz thickness monitor mounted inside the dilution refrigerator. In Fig. 2, we plot R_{\square} versus $1/T^{1/2}$ measured on two Be film sections 2 mm apart, following a sequence of evaporations to increase the thickness of the film. The two curves at the top of Fig 2(a) were measured for two very thin film thicknesses (5-6 Å) before Mn was evaporated. These samples displayed the typical upward curvature for insulating films as seen in Fig 1 as well as the previously reported large and negative magnetoresistance [16]. We then evaporated a small amount of Mn impurities onto the Be film by manually opening the shutter briefly. We observe in Fig. 2(a) that the upturn in the R_{\square} , versus $1/T^{1/2}$ curve disappeared after Mn impurities were introduced (Curve 3 from the top), recovering a rather clean Efros-Shklovskii hopping behavior. In addition, the large negative magnetoresistance observed earlier [16] also disappeared. Such behavior persists for films produced following subsequent Be evaporation steps to increase the thickness, as shown by the remaining curves in Fig. 2. We believe this is strong evidence that the large and negative magnetoresistance observed in the absence of Mn impurities is due to the field-suppression of superconductivity [18].

The high temperature data in Fig. 1 and the data with Mn impurities in Fig. 2 converge to a unique resistance pre-factor of $R_0 \approx 10 \text{ k}\Omega/\square$ in the $T \rightarrow \infty$ limit, which is close to a pre-factor of $R_0 \sim R_Q/2 = (h/e^2)/2 \approx 13 \text{ k}\Omega/\square$ for the ES hopping law $R_{\square}(T) = R_0 \exp(T_0/T)^{1/2}$ with $T_0 = 2.8e^2/(4\pi\epsilon_0 k_B \xi_L \kappa)$, where e is electron charge, ϵ_0 is the vacuum permittivity, and k_B is the Boltzmann constant. This hopping law is predicted for the ES soft Coulomb gap [19] in the density of states (DOS). We fit all our data to the ES hopping law to obtain parameters T_0 and R_0 . We use the sheet resistance of the films at 20 K, R , as the disorder parameter. The convergence of the curves seen in Fig. 1 is significant in that it is observed for all the films that are either insulating or in the vicinity of the SI transition, with R varying by nearly three orders of magnitude as shown in the lower frame of Fig. 2. Using T_0 , we obtain the product, $\xi_L \kappa = 2.8e^2/4\pi\epsilon_0 k_B T_0$. In Fig. 3, $\xi_L \kappa$ and R_0 are plotted versus R .

Next, we use the measured tunneling DOS, shown in Fig 4 for one of the samples in Fig. 2, to obtain κ , so that ξ_L can be extracted from the product $\xi_L \kappa$. The predicted [19] linear DOS is given by $N(E) = [\alpha(4\pi\epsilon_0 \kappa)^2/e^4]|E|$ with a slope of $\alpha(4\pi\epsilon_0 \kappa)^2/e^4$, where α is on the order of unity and E is energy measured from the Fermi energy. In practice, we

use Al/Al₂O₃/Be junctions to measure the tunneling conductance G as a function of the bias voltage, V_{bias} . We then calculate the slope of the measured linear G -versus- V_{bias} curve, which is proportional to κ^2 since G is proportional to the DOS. Using the slopes calculated from the tunneling conductance for samples of varying R , we have obtained a power-law dependence of $\kappa^2 \sim R^{-1.73 \pm 0.10}$, or, $\kappa \sim R^{-0.87}$. The absolute value of κ is unknown, since we have not attempted to convert G to the DOS in real units. This conversion requires a calibration factor that is related to the product of the tunneling probability and the DOS of the Al counter-electrode. This calibration factor should be a constant for a given junction in the relevant temperature regime. We divide the product $\xi_L \kappa$ by κ ($\sim R^{-0.87}$) to extract ξ_L . Since the absolute value of κ is unknown, the value of ξ_L so obtained also carries an unknown constant factor. However, it is reasonable to set ξ_L to a value of $\xi_{L0} = 5 \text{ \AA}$ in the extreme insulating limit ($R = 10^3 - 10^4 \text{ k}\Omega/\square$). We believe that this assumption is correct up to a numerical factor of 2 [20]. Following these steps, we have obtained ξ_L as a function of the disorder parameter R , as shown in Fig. 5. With the absolute value of ξ_L set, we divide the product $\xi_L \kappa$ by ξ_L to set the absolute value for κ , which is plotted in the inset to the upper frame of Fig. 3. With this procedure, ξ_L and κ are determined, *independently*, with an uncertainty factor of about 2. The scaling theory of localization in 2D predicts in the weakly disordered limit that ξ_L grows exponentially with decreasing disorder [1,7]: $\xi_L = l \exp[(\pi/2)k_F l]$, where k_F is the Fermi wave number and l is the elastic mean free path. In deriving this, the relation for conventional transport, $R = (h/e^2)(1/k_F l) \approx (26 \text{ k}\Omega)(1/k_F l)$, is used. This scaling theory is a perturbative expansion based on $1/k_F l$. We note that, effectively, the value of $k_F l$ crosses 1 for films of $R \sim 26 \text{ k}\Omega/\square$. One may assume that not too far from $k_F l = 1$ the theory is still relevant to certain degree. Bearing this in mind and assuming $l \approx \xi_{L0}$ for films of $k_F l \leq 1$, we rewrite the expression for ξ_L : $\xi_L = l \exp[(\pi/2)(h/e^2)/R] \approx \xi_{L0} \exp[(\pi/2)(h/e^2)/R]$. We plot this relation as a solid curve in Fig. 5. The agreement between the data and the solid line is surprisingly good, as there is no adjustable parameter.

The SI transition in the Be films occurs at a critical resistance of $R \approx 11.7 \text{ k}\Omega/\square$, as indicated by the dashed line in Fig. 5. Now, we show that the transition occurs just as ξ_L crosses ξ_S . We estimate the value of ξ_S using the Ginzburg-Landau expression [21], ξ_S

$= 0.855(\xi_0 l)^{1/2}$. The BCS coherence length is $\xi_0 = \hbar v_F / (\pi \Delta_0) = \hbar v_F / (1.76 \pi k_B T_C) = 0.18 \hbar v_F / (k_B T_C)$, where Δ_0 is the BCS gap energy for $T = 0$ and v_F is the Fermi velocity which is related to R by $R = (h/e^2)(1/k_F l)$. Based on the superconducting transition temperature $T_C \approx 7.0$ K for thick films of $R \sim 2$ k Ω/\square , ξ_S is estimated to be 150 Å. Comparing this value of ξ_S with ξ_L in Fig. 5, we conclude that the SI transition occurs just as ξ_L crosses ξ_S . We note that a direct comparison between Δ_L and Δ_S is difficult [20]. To estimate Δ_L near the SI transition, we use a free-electron model: $\Delta_L = [N(0)\xi_L^d]^{-1} = (a^2 E_F) / \xi_L^2$, where $a \sim 1$ Å is the atomic spacing, $E_F \sim 10^4$ K is the Fermi energy, and $d = 2$. This leads to a lower bound of 1 K for Δ_L . The actual value for Δ_L should be higher since the DOS at the Fermi energy is significantly depressed from the free-electron result for films near the SI transition. Alternatively, one may argue that the characteristic energy of the insulating phase, $k_B T_0$, is in fact a reasonable measure of Δ_L . In Fig. 5, we plot T_0 and T_C for Be films of varying R . The T_C values were obtained from two film sections of varying thickness, with the SI transition occurring at a critical resistance of 11.7 k Ω/\square . Here we observe that the SI transition occurs as T_0 becomes comparable to T_C .

In summary, we have determined, *independently* and up to a constant on the order of unity, the localization length, ξ_L , and the dielectric constant, κ , for quench-condensed ultrathin amorphous beryllium films. ξ_L decreases exponentially with increasing disorder. Our data suggest that the SI transition occurs when ξ_L crosses the Ginzburg-Landau coherence length, ξ_S . We gratefully acknowledge discussions with A. M. Goldman, Z. Ovadyahu, and I. Zharekeshev. This work was supported in part by NSF under Grant No. DMR-0551813.

References

1. P. A. Lee and T. V. Ramakrishnan, *Rev. Mod. Phys.* **57**, 287 (1985); D. Belitz and T. R. Kirkpatrick, *ibid.* **66**, 281 (1994).
2. R. C. Dynes, J. P. Garno, and J. M. Rowell, *Phys. Rev. Lett.* **40**, 479 (1978); D. B. Haviland, Y. Liu, A. M. Goldman, *ibid.* **62**, 2180 (1989); H. M. Jaeger, D. B. Haviland, B. G. Orr, and A. M. Goldman, *Phys. Rev. B* **40**, 182 (1989); A. M. Goldman and N. Markovic, *Phys. Today*, **51**, No. 11, 39 (1998); J. M. Valles, Jr., R. C. Dynes, J. P. Garno, *Phys. Rev. Lett.* **69**, 3567 (1992); S.-Y. Hsu, J. A. Chervenak, and J. M. Valles, Jr., *Phys. Rev. Lett.* **75**, 132 (1995).
3. A. F. Hebard and M. A. Paalanen, *Phys. Rev. Lett.* **65**, 927 (1990).
4. M. P. A. Fisher, G. Grinstein, S. M. Girvin, *Phys. Rev. Lett.* **64**, 587 (1990); M. P. A. Fisher, *ibid.* **65**, 923 (1990).
5. S. Sondhi, S. Girvin, J. Carini, and D. Shahar, *Rev. Mod. Phys.* **69**, 315 (1997).
6. P. W. Anderson, *J. Phys. Chem. Solids* **11**, 26 (1959).
7. E. Abrahams, P. W. Anderson, D. C. Licciardello, and T. V. Ramakrishnan, *Phys. Rev. Lett.* **42**, 673 (1979).
8. A. Kapitulnik and G. Kotliar, *Phys. Rev. Lett.* **54**, 473 (1985); G. Kotliar and A. Kapitulnik, *Phys. Rev. B* **33**, 3146 (1986).
9. M. Ma and P. A. Lee, *Phys. Rev. B* **32**, 5658 (1985).
10. Y. Imry and M. Strongin, *Phys. Rev. B* **24**, 6353 (1981); Y. Shapira and G. Deutscher, *ibid.* **27**, 4463 (1983); A. Frydman and Z. Ovadyahu, *ibid.* **55**, 9047 (1997).
11. Y. Liu *et al.*, *Phys. Rev. Lett.* **67**, 2068 (1991).

12. N. Mason and A. Kapitulnik, Phys. Rev. Lett. **82**, 5341 (1999).
13. N. Markovic *et al.*, Phys. Rev. B **60**, 4320 (1999).
14. E. Bielejec and W. Wu, Phys. Rev. Lett. **88**, 206802 (2002).
15. F. W. Van Keuls *et al.*, Phys. Rev. B **56**, 13263 (1997); M. Furlan, *ibid.* **57**, 14818 (1998); F. Hohls, U. Zeitler, and R. J. Haug, Phys. Rev. Lett. **88**, 036802 (2002).
16. E. Bielejec, J. Ruan, and W. Wu, Phys. Rev. B **63**, R100502 (2001).
17. E. Bielejec, J. Ruan, and W. Wu, Phys. Rev. Lett. **87**, 036801 (2001).
18. G. Sambundamurthy, L. W. Engel, A. Johansson, and D. Shahar, Phys. Rev. Lett. **92**, 107005 (2004).
19. B. I. Shklovskii and A. L. Efros, *Electronic Properties of Doped Semiconductors* (Springer, New York, 1984).
20. D. Shahar and Z. Ovadyahu, Phys. Rev. B **46**, 10917 (1992).
21. M. Tinkham, *Introduction to Superconductivity* (New York, McGraw Hill, 1996).

Figure Captions

Fig. 1 Selected curves of R_{\square} versus $1/T^{1/2}$ for one Be film section following deposition steps to increase film thickness (from top to bottom). The thickness for these films changed from 4.6 Å to about 10 Å. The straight lines are drawn as a guide for eye, showing that in the high-T regime all the curves follow straight lines that converge to about 10 k Ω/\square in the $T \rightarrow \infty$ limit. The films for bottom curve is superconducting at low temperatures.

Fig. 2 Upper frame: R_{\square} versus $1/T^{1/2}$ for one Be film section following a sequence of evaporation steps. After the second curve from the top were measured, Mn impurities were evaporated onto the film, which resulted in the third curve from the top. Other curves resulted from additional Be evaporation steps. Lower Frame: Same data from the frame plotted on a broader temperature range.

Fig. 3 The product $\xi_L \kappa$ and R_0 are plotted versus the disorder parameter R . Data points shown here were obtained on forty-one films of various thickness fabricated in four experimental runs. The dielectric constant κ , with its absolute value fixed as described in the main text, is plotted in the inset to the upper frame.

Fig. 4 Tunneling conductance versus the bias voltage measured at 3 K on one Be film section in Fig. 2, showing the linear DOS near the Fermi energy. Curves from the bottom to the top correspond to values of the disorder parameter $R = 3740, 298, 119, 37.3,$ and 14.3 k Ω , respectively.

Fig. 5 The localization length, ξ_L , is plotted as a function of the disorder parameter R . The absolute value of ξ_L is fixed at $\xi_{L0} = 5$ Å in the extreme insulating limit. The solid curve is for $\xi_L = \xi_{L0} \exp[(\pi/2)(h/e^2)/R]$. The dashed line indicates the critical resistance for the zero-field SI transition, separating the superconducting phase on the left from the insulating phase on the right.

Fig. 6 The parameter T_0 (solid circles) from fits to the ES hopping law and the measured superconducting transition temperature T_C are plotted versus the disorder parameter R . Up and down triangles represent data from two different experimental runs. The critical sheet resistance is $11.7 \text{ k}\Omega/\square$ as indicated by the dashed line.

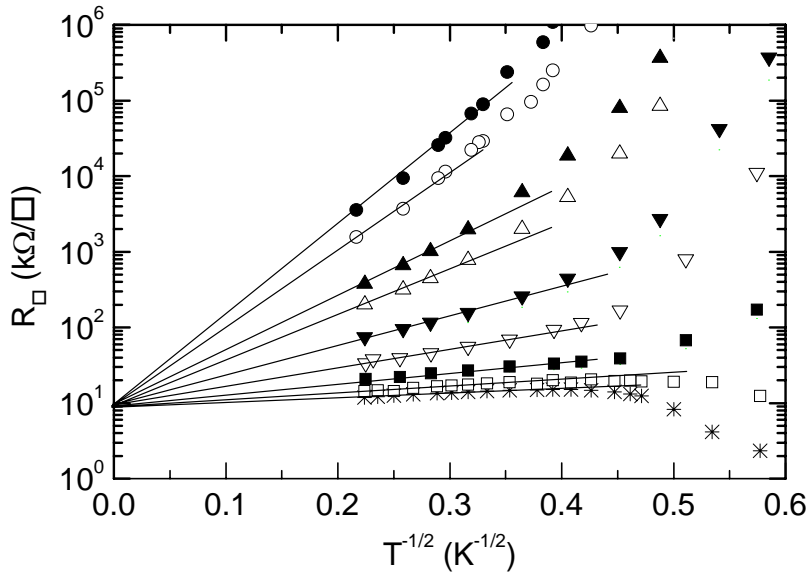


Figure 1 W. Wu et al.

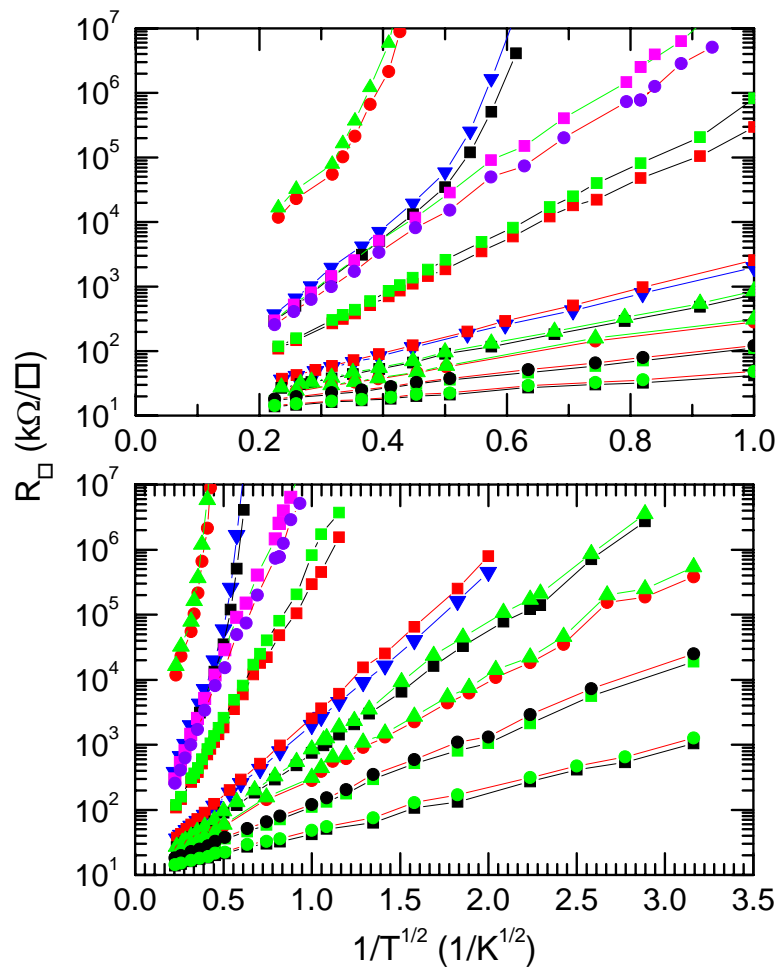


Fig. 2

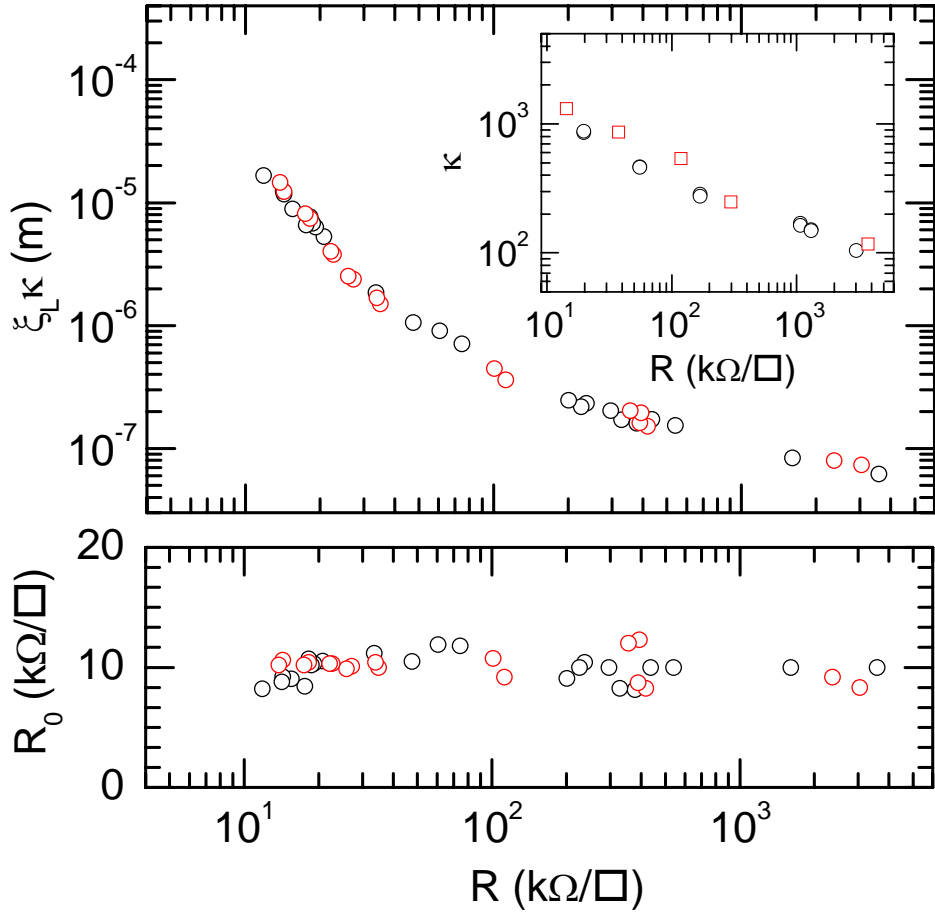


Figure 3 W. Wu et al.

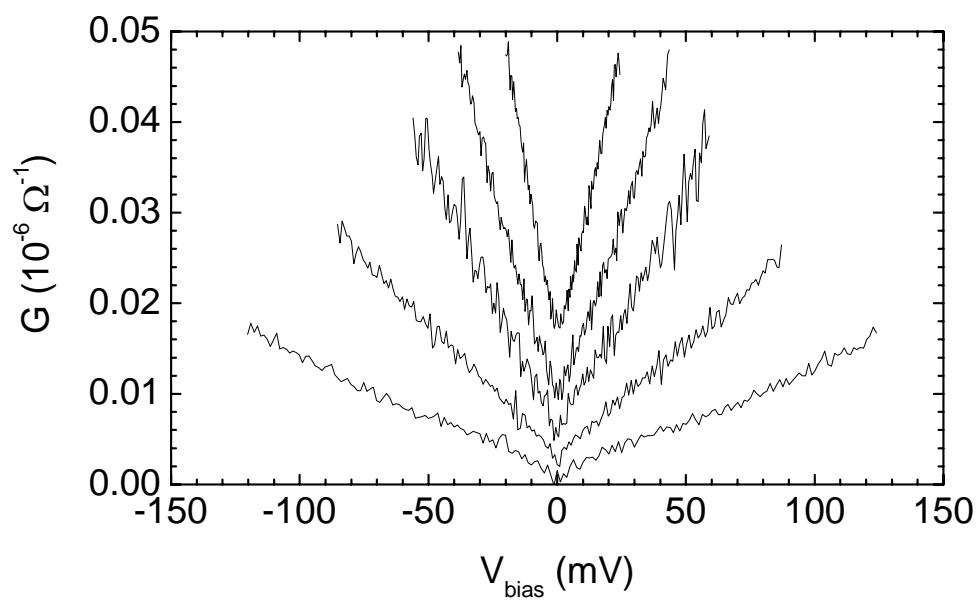


Fig. 4 W. Wu et al.

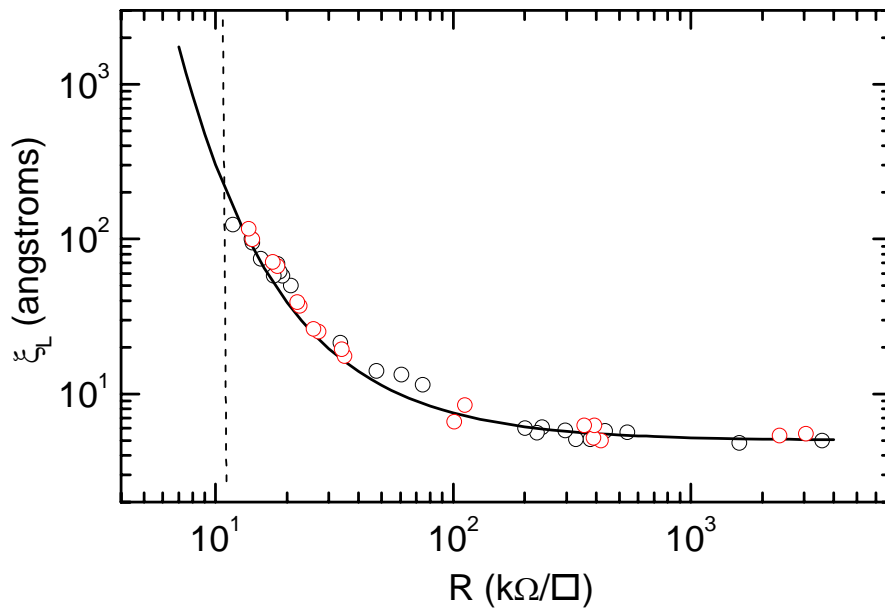


Figure 5 W. Wu et al.

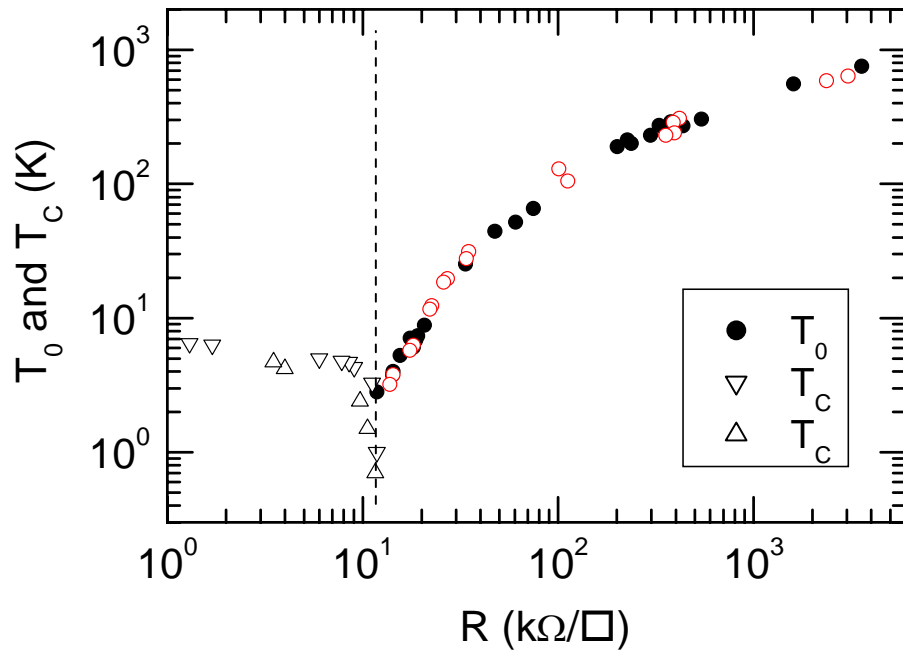


Figure 6 W. Wu et al.